J. N. Am. Benthol. Soc., 2003, 22(1):143–151

A low-cost sensor for measuring spatiotemporal variation of light intensity on the streambed

BRETT A. MELBOURNE[1]

Division of Botany and Zoology, Australian National University, Canberra, ACT 0200, Australia

PAUL J. DANIEL

CSIRO Land and Water, GPO Box 1666, Canberra, ACT 2601, Australia

Abstract. We describe a low-cost sensor for measuring light intensity on the streambed that is simple and quick to construct. We also describe an amplifier circuit for use with the sensor. The sensor consists of a photodiode and diffuser encased in heat-shrink tubing. The sensor had acceptable spectral and cosine responses, a good linear relationship with a Li-Cor Quantum sensor, and withstood the rigors of the streambed environment. The low cost of the sensor makes it suitable for studies of spatiotemporal variation, where many sensors are required. In a field trial of the sensors conducted simultaneously at 10 sites, we characterized variation at a range of spatial scales and found a peak in the variance between 1-m plots within a site.

Key words: light sensor, photosynthetically active radiation, measurement, streams, heterogeneity, amplifier circuit.

Photosynthetically active radiation (PAR) is an important variable that directly affects primary productivity on the streambed (Vannote et al. 1980, Feminella et al. 1989, Wootton and Power 1993, Hill et al. 1995). In this environment, PAR can have high spatial and temporal variation because 1) topography and riparian vegetation form a complex horizon, 2) PAR is attenuated by the water column, and 3) solar angle and cloudiness change diurnally and seasonally (Hill 1996). To characterize this variation, replicated observations at multiple spatial and temporal scales are required (Cooper et al. 1997). However, current systems for monitoring PAR on the streambed are too expensive to achieve adequate replication in studies of spatiotemporal variation. A suitable sensor must be inexpensive, easy to construct and sensitive to light in the photosynthetically active spectrum. In addition, the sensor must be able to withstand the rigors of the underwater environment and frequent high-flow events. Gutschick et al. (1985) described a PAR monitoring system that used small, leaf-mounted photodiodes to simultaneously measure PAR at up to 32 points in a vegetative canopy. We developed a similar system for measuring PAR at multiple points on the streambed. The cost of the sensor described here was <AUS$8 (US$6) in 1997, for all components and cabling. We also describe an amplifier circuit of low cost for use with the sensors.

[1] Present address: Section of Evolution and Ecology, University of California, Davis, California 95616 USA. E-mail: bamelbourne@ucdavis.edu

PAR Sensor

Construction

The sensor consists of a blue-sensitive photodiode and a plastic diffusing disc encased in heat-shrink tubing (Fig. 1). The diffusing disc (6 mm diameter, 5 mm height) was cut from a flat sheet of acrylic opal (Plexiglas GS 059, Rohm and Haas, Philadelphia, Pennsylvania) using a drill-mounted tool. Apart from this cutting step, the sensor was very simple to construct and required <10 min of labor per sensor. After soldering the cable (PVC insulated, 0.2 mm, stranded copper, up to 20 m long) to the photodiode, a clear sleeve of heat-shrink tubing (6.4 mm diameter, 35 mm long, nonadhesive) was positioned over the diode pins and filled with silicon sealant (neutral cure) using a syringe. The tubing was then shrunk slightly so that the sealant completely encased the pins and a short section of cable, rendering the base of the unit waterproof. After allowing the sealant to cure, the diffusing disc was placed on top of the diode and encased in black adhesive-lined heat-shrink tubing (6.4 mm diameter). The black tub-

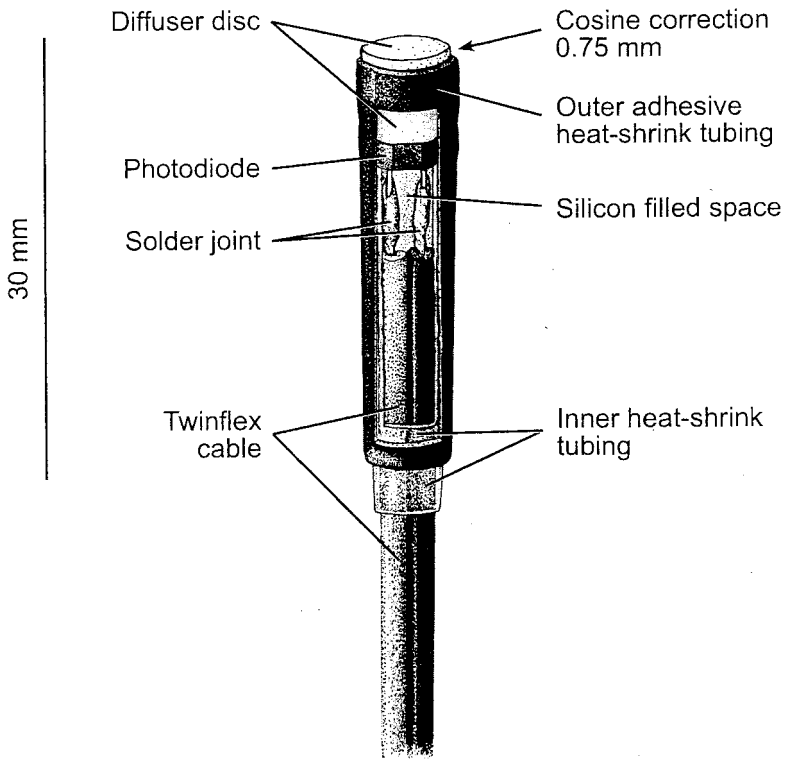

FIG. 1. Sketch of the sensor showing the internal and external structure. The black, outer heat-shrink tubing encases the sensor. In the figure, a window in the outer heat-shrink tubing has been cut away to reveal the inner structure of the sensor. The inner heat-shrink tubing has also been cut away. The inner heat-shrink tubing, filled with silicon sealant, encases the solder joints and extends to the base of the diode.

ing was then trimmed 0.75 mm back from the lip of the diffuser to partially correct the cosine response.

Spectral characteristics

A PAR sensor should be sensitive to light in the 400 to 700 nm range and approximate an ideal quantum response (Biggs et al. 1971). We used CBC-2014CF photodiodes from Centrovision Incorporated, Newbury Park, California. These photodiodes are sensitive in the blue range, as required, but compared to the ideal quantum response, underestimate at shorter and longer wavelengths (Fig. 2). The diffuser provided a sharp cutoff at 400 nm and transmitted light equally (50%) at other wavelengths. According to Centrovision's specifications, the photodiode has very low temperature dependence and a short response time (10–90% in <10 μs). Gallium arsenide phosphide (GaAsP) photodiodes have been suggested as an alternative (Gutschick et al. 1985, Pontailler 1990). Compared to a GaAsP diode, the 2014CF is slightly more sensitive at short wavelengths and decreases in sensitivity more gradually at long wavelengths (Fig. 2). Either photodiode will produce some bias in understory PAR measurements if the sensor is calibrated under sunlight in the open (Pearcy 1989). A 3 to 4% bias has been estimated for the GaAsP diode (Chazdon and Fetcher 1984). The addition of a blue filter to either diode improves the spectral response and reduces this bias (Pontailler and Genty 1996. V. P. Gutschick, New Mexico State University, Las Cruces, New Mexico, personal communication). We attempted to install a gelatin filter between the diffuser and diode (Kodak Wratten No. 80B) but the heat needed to install the heat-shrink tubing destroyed the filter. Nevertheless, without a filter, either the 2014CF or a GaAsP diode is adequate for most heterogeneity studies, particularly when the expected variation in light intensity is large relative to the

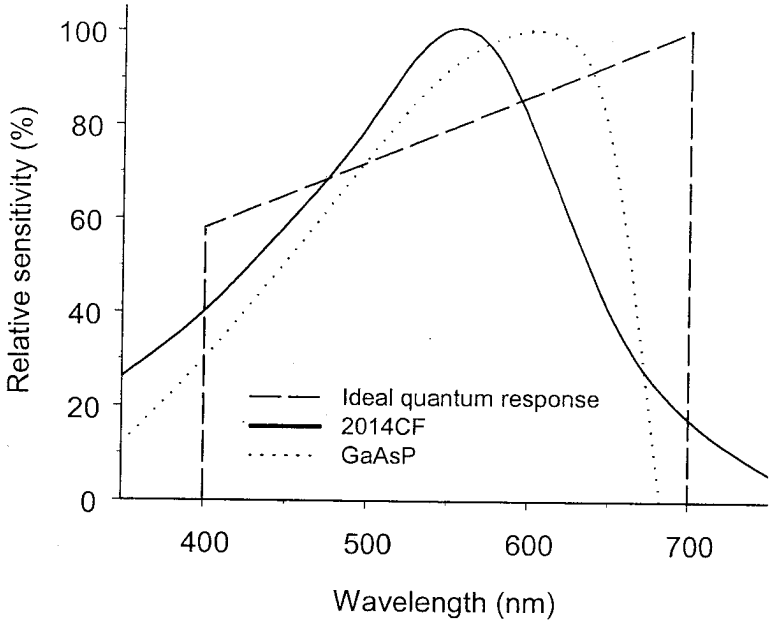

FIG. 2. Spectral response of the Centrovision CBC-2014CF photodiode compared to the ideal quantum response, and a gallium arsenide phosphide (GaAsP) photodiode (G1117, Hamamatsu Photonics, Hamamatsu, Japan). Spectral responses are from manufacturer's specifications. The Li-Cor LI190 SA Quantum sensor approximately follows the ideal quantum response. For the constructed sensor, the diffuser provides a sharp cutoff at 400 nm.

spectral bias. In addition, variation in light intensity is probably much more important to the photosynthetic response of aquatic algae than spectral quality (Hill 1996). A glass filter could be used if greater accuracy were required but this addition would increase the cost of the sensor (Pontailler and Genty 1996).

Cosine response

The cosine response of the sensor was measured using collimated light, as described in Biggs et al. (1971). The error of the cosine response was <2.1% up to a zenithal beam angle of 75° (Fig. 3). However, the compensation provided by the exposed vertical edge of the diffuser was too great at ≥75°. The cosine error at angles >75° in standard cosine-corrected heads, such as the LI190 SA (Li-Cor Limited, Lincoln, Nebraska), is limited by the addition of an outside rim (Biggs et al. 1971). However, adding an outer rim greatly complicates the construction of a PAR sensor, and the error from omitting the outside rim is inconsequential for most work on the streambed. Provided that sensors are installed horizontally, angles of incidence >75° are rarely encountered because of micro- and macrotopographic shading. In addition, irradiances are low at high angles of incidence (early morning and late evening), and the relative errors shown in Fig. 3 translate to small absolute errors (e.g., bias equals +25 μmol s^{-1} m^{-2} at 75° incidence in midsummer at Canberra, Australia, lat 35°17′S, long 149°08′E). These errors are even smaller if daily integrated PAR is the quantity of interest (e.g., bias equals +0.01% of daily total for a clear, midsummer day at Canberra).

Amplifier Circuit

The current generated by the sensors is converted to a voltage when they are wired in parallel with a precision resistor (~1 KΩ). This signal is in the order of millivolts and can be measured directly by many dataloggers. However, to avoid nonlinearity, the exact resistor value depends critically on the sensitivity of an individual diode and the anticipated light intensity to be measured. Also, such a signal is too small to be measured by many less-expensive datalog-

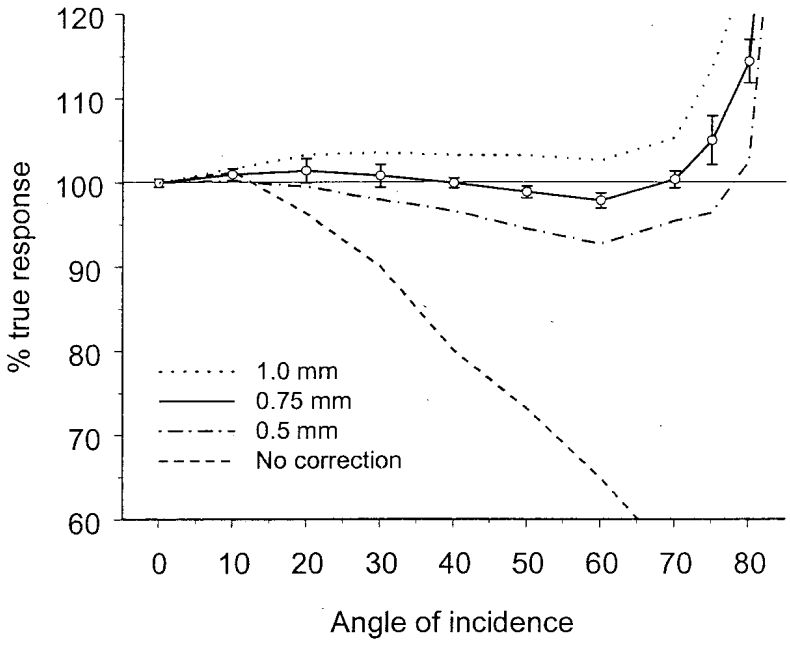

FIG. 3. Cosine response (mean ± SE, n = 4) of the sensor, corrected by exposing the vertical edge of the diffuser by 0.75 mm. Responses for an uncorrected sensor and sensors with 0.5 mm and 1.0 mm vertical edge of diffuser exposed are also shown. The 100% true response is the response predicted by the cosine curve.

gers or analog-to-digital converters that require an input level of several volts.

We constructed an amplifier circuit (Fig. 4) to convert the sensor current to a voltage output suitable for the dataloggers we used, which required an input of 0 to 5 V. The circuit allows light intensity to be measured with excellent linearity over several orders of magnitude. The amplifier, configured as a precision current-to-voltage converter, provides an output of 160 mV/μA on high range and 1.5 V/μA on low range. High range is suitable for measuring instantaneous light levels up to 3500 μmol s^{-1} m^{-2}. The precision of measurements depends on the datalogger used. Our dataloggers used an 8-bit analog-to-digital converter, which provided poor precision at low light levels using the high-range circuit (precision of datalogger only, not including errors from other sources: ±13% at 100 μmol s^{-1} m^{-2} compared to ±1% at 1300 μmol s^{-1} m^{-2}). For increased amplification of the signal in low light conditions, such as in deep shade, the low-range circuit is suitable for measuring instantaneous light levels up to 350 μmol s^{-1} m^{-2}. The low-range circuit provided a 10-fold increase in precision for our dataloggers (±1.3% at 100 μmol s^{-1} m^{-2}). An alternative solution to increasing the precision would be to use a datalogger with a more sensitive analog-to-digital converter (e.g., 12 bit). Components for the circuit were selected for their low power consumption and stable electrical characteristics over changes in temperature. The cost of the components in the basic circuit was AUS$7 (US$5) for the power supply (comprising 1 voltage regulator and 1 voltage converter) and AUS$6 (US$4) for 1 amplifier module. Battery life using 8 C-size alkaline cells was ~1000 h of continuous operation for a circuit comprising 1 power supply and 2 amplifiers. An alternative amplifier circuit is described by Biggs et al. (1971).

The basic circuit in Fig. 4 can be modified in various ways. For example, we used 1 power supply and 2 amplifier modules (1 high range and 1 low range) together with a multiplexing unit. With this modification, we could run 8 sensors connected to the same circuit and monitor each sensor at 4-min intervals with a dual range of amplification to allow for high and low light conditions, or we could run 16 sensors, 8 each on high and low range. Greater precision could be achieved under extremely low light conditions by increasing the signal amplification, by

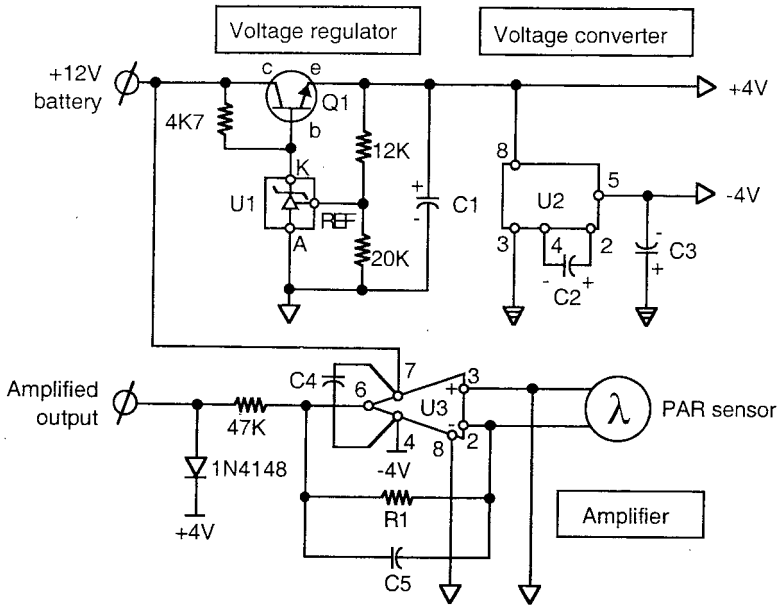

FIG. 4. A basic amplifier circuit for use with the photosynthetically active radiation (PAR) sensor. The basic circuit has 3 modules: a voltage regulator and a voltage converter (which together make up the power supply) and the amplifier itself. Capacitors: C1 4.7 μF electrolytic, C2–3 22 μF tantalum, C4 0.1 μF polyester, C5 Phillips 378 series polypropylene (high range 1 μF, low range 0.1 μF). Resistors: R1 high range 160 KΩ, low range 1.5 MΩ. All resistors are metal film type with 1% tolerance. Other components: Q1 BC337 transistor, U1 TL431 voltage regulator, U2 7660 DC-DC voltage converter, U3 TLC 2201CP chopper-stabilized operational amplifier. The 1N4148 diode and 47 KΩ resistor provide protection for the datalogger inputs when the amplifier is overloaded on low range. These components are omitted from the high-range circuit. C5 provides low-pass filtering for signals >10 Hz, and is optional. We installed C5 to prevent interference from other electronic equipment installed at the site.

increasing the value of resistor R1 (Fig. 4). Short-term changes, such as sunfleck activity, could be monitored using 1 amplifier module per sensor with a short logging interval (e.g., 1–60 s).

Calibration

The sensors were calibrated against a Li-Cor LI190 SA Quantum sensor. Measurements were made on a roof top at regular intervals over a full day, in natural daylight, with a clear sky and with an unobscured horizon (Canberra, Australia). We calibrated the sensor and tested its cosine response in air because the calibration of similar sensors was not affected in air compared to under water (Dawson 1981) and calibration under water was inconvenient. We used DS90 dataloggers (Dataflow Systems, Noosaville, Queensland, Australia) to record the amplified sensor output on an 8-bit digital scale. A Li-Cor LI1000 datalogger was used to record the output from the Li-Cor sensor. There was an excellent linear relationship between the sensors and the Li-Cor LI190 SA across the range of light levels and for both levels of amplification (Fig. 5). Slopes varied among sensors (Fig. 5, $p < 0.001$), so each sensor must be calibrated individually. The calibrations suggest good precision over a wide range of light conditions. The 95% confidence interval for a new observation (i.e., 95% prediction interval) for PAR was never larger than ±25.2 μmol s^{-1} m^{-2} on high range and ±4.6 μmol s^{-1} m^{-2} on low range (Fig. 5). Also, the calibration error was small compared to spatial variation in PAR (see below). According to the manufacturer's specifications, the photodiode and diffuser have good long-term stability with exposure to sunlight, and sensors using similar components showed only small calibration drift over 2 y of continuous operation (Pontailler and Genty 1996).

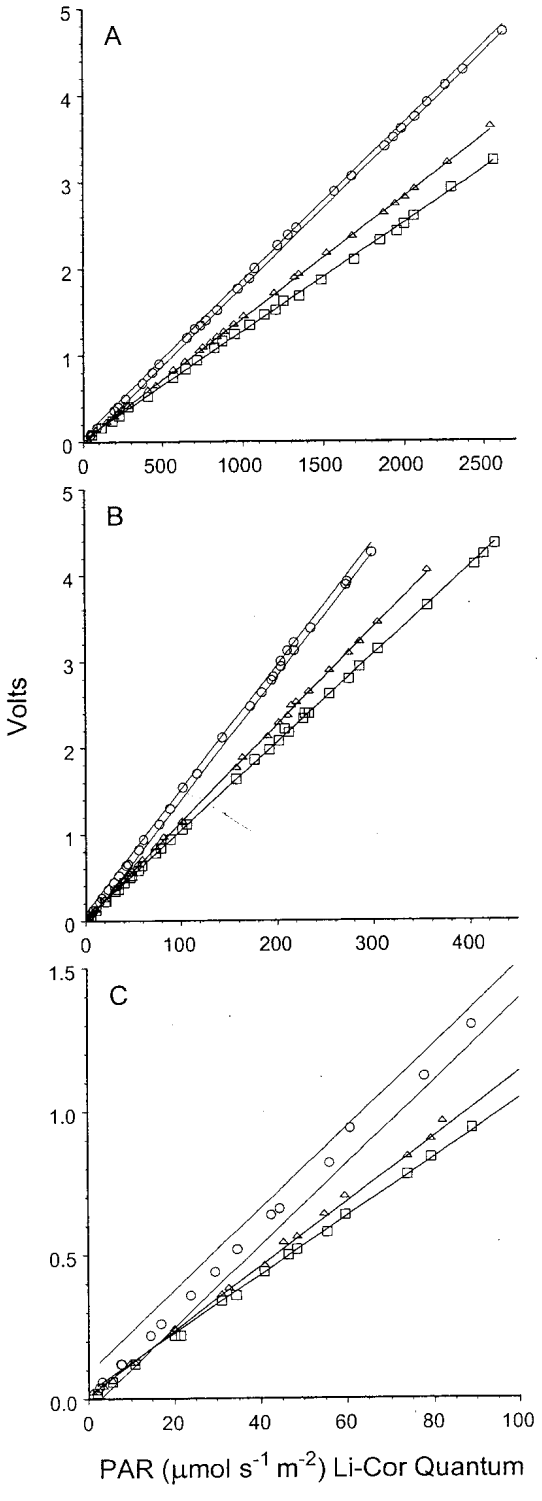

FIG. 5. Voltage output from 3 sensors (different symbols) at high- (A) and low-range (B) amplification versus photosynthetically active radiation (PAR) measured with a Li-Cor LI190 SA Quantum sensor. Symbols represent the same sensor in each panel. Fitted lines are from linear regression ($R^2 > 0.999$ for all regressions), with the exception of the sensor represented by circles, for which 95% prediction intervals are shown. Panel C is an enlargement of the low-range data (B) to show detail at low irradiance.

TABLE 1. Scales of variation in photosynthetically active radiation (PAR): variance components of ln-transformed PAR (Var(lnPAR)), effective degrees of freedom (df), % of total variance on the ln-transformed scale (% Var), and coefficients of variation back-transformed to the natural scale (CV(PAR)).

Scale	Var(lnPAR)	df	% Var	CV(PAR)
Instantaneous PAR at noon				
Site	0.3024	8.79	37.2	0.594
Time	0.3450	28.32	42.5	0.642
10 m[a]	0.0000	6.69	0.0	0.000
Plot	0.1544	11.19	19.0	0.409
Rock	0.0107	2.00	1.3	0.104
Daily integrated PAR				
Site	0.4924	9.00	72.0	0.798
10 m	0.0453	9.99	6.6	0.215
Plot	0.0989	19.85	14.5	0.322
Rock	0.0470	19.16	6.9	0.219

[a] The estimated variance component at the 10 m scale was −0.0047. This small, negative variance component was assumed equal to 0 (difference from 0, $p = 0.97$, likelihood ratio test) and the random-effects model was fitted omitting the 10 m term (Payne 2000)

Field Trials

We have used the sensors to monitor solar radiation on the streambed at 10 sites simultaneously, with up to 16 sensors per site and for periods of up to 3 wk. We drilled holes, 10 mm in diameter and 30 mm deep, into stream cobbles to install the sensors on the streambed. About 30 s were required to drill each hole using a cordless, hammer-action drill. The sensors were positioned in the cobble holes so that the vertical edge of the diffuser was exposed and the top of the diffuser was horizontal. The cable was secured to the cobble with a 20 mm band of rubber (automobile tire inner tube) and buried in the streambed. Cable lengths of 15 to 20 m enabled us to position dataloggers above the high-flow mark and to monitor sections of

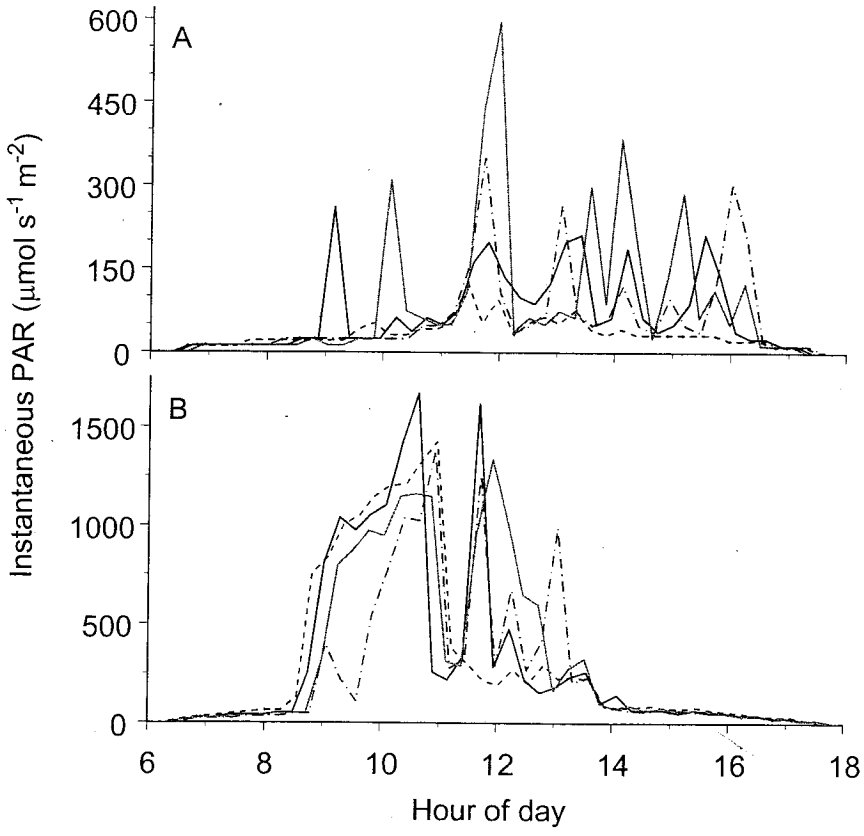

FIG. 6. Spatiotemporal variation in photosynthetically active radiation (PAR) over 1 d (8 April 1997), for 2 sites (A and B), on the Bimberamala River. Lines are the traces for 4 sensors at different locations within each site, logged at 16-min intervals.

stream up to 20 m in length using 1 datalogger. We encountered few problems with this setup and found it particularly convenient for remote field sites. Installation of the sensors in stream cobbles and the resulting low profile of the sensors in the current meant that debris rarely obstructed the sensor. Sensors were not disturbed by high-flow events that did not move the streambed. In larger events, in which the streambed was disturbed, sensors were typically ejected from their installation but few were damaged.

Spatial variation in PAR

As an example of the spatial variability encountered in streams, we provide data from 10 sites monitored simultaneously over 1 d (8 April 1997) in southeastern New South Wales, Australia (lat 35°23′S, long 150°10′E). We monitored PAR at 5 sites in each of two 4th-order tributaries (Bimberamala and Yadboro Rivers) of the Clyde River. The catchments of both rivers are mountainous (max. altitude 800 m, min. altitude 50 m) and vegetated with wet sclerophyll forest that extends to the riparian zone. The sites were spread along 10 km sections of each tributary and encompassed a range of solar-radiation regimes. Each site was a 20 m length of stream. Within each site, we used a hierarchical sampling design to measure variance at 3 spatial scales nested within the site scale. Each site was divided into 2 lengths of 10 m (10 m scale), and from each 10 m length we selected 2 plots of 1 m by 1 m (plot scale) at coordinates determined by a random number draw. Within each 1 m plot, we selected 1 rock at random in which to install a sensor. In plots nested within 1 of the 10 m lengths, we selected a 2nd rock in a random direction and 1 m distant from the 1st rock

(rock scale). In total, there were 6 sensors at each site, which we logged at 16 min intervals on high range. Our datalogger setup included 3 logging times, 2 min apart, within each 16 min period (i.e., at 0, 2, and 4 min), with 2 sensors logged on separate channels at each of these times.

We estimated variance components at different spatial scales for instantaneous PAR at noon and for daily integrated PAR using restricted maximum likelihood (Genstat, release 4.21, Lawes Agricultural Trust, Rothamsted Experimental Station, UK), after first transforming the data by natural logarithms. We calculated the % contribution of each (j^{th}) scale to the total variance from all (i) scales as $100 \times \sigma^2_j / \Sigma\sigma^2_i$, where σ^2 is the estimated variance component on the log-transformed scale (Underwood and Chapman 1996). We calculated coefficients of variation (CV) on the natural scale as $\sqrt{e^{\sigma^2} - 1}$ (Johnson et al. 1994). For instantaneous PAR at noon, time was nested within site and the 10 m and lower spatial scales were nested within time. This nested specification ensured that the variance between the 3 logging times (within the 16 min period at noon) was separated from the spatial variances.

Considerable variation between sites and between sensors within a site was observed in instantaneous PAR (Fig. 6). Of the spatial scales within a site, the variance component at the plot scale was greatest for both PAR at noon and daily integrated PAR, with much less contribution from rock and 10 m scales (Table 1). The small contribution of the rock scale compared to higher scales is noteworthy because calibration error is included in the variance component at this scale, suggesting that calibration error is small relative to variance at larger spatial scales. Out of the total variance at all spatial scales, the within-site variance amounted to 35% for PAR at noon and 28% for daily integrated PAR. This observation, and the high CV at the plot scale (Table 1), suggests that a single sensor would not be representative for multiple plots within a site. Similarly, using multiple sensors would reduce the uncertainty in mean PAR at the site scale. Variation at the plot scale likely arises from shading by riparian vegetation and might be characteristic of forested streams.

In conclusion, there is a tradeoff between the accuracy and cost of individual sensors for applications requiring many sensors, such as in studies of spatiotemporal variation. The sensors described here have sufficient accuracy for many applications in stream ecology and are inexpensive and easy to construct. They also have proved to withstand the rigors of the streambed environment and cost little to replace if they are damaged.

Acknowledgements

We thank V. Gutschick, J. Pontailler, and T. Murphy for their helpful advice and Sharyn Wragg for the sensor illustration. BAM was supported by an Australian Postgraduate Award.

Literature Cited

BIGGS, W. W., A. R. EDISON, J. D. EASTIN, K. W. BROWN, J. W. MARANVILLE, AND M. D. CLEGG. 1971. Photosynthesis light sensor and meter. Ecology 52: 125–131.

CHAZDON, R. L., AND N. FETCHER. 1984. Photosynthetic light environments in a lowland tropical rain forest in Costa Rica. Journal of Ecology 72: 553–564.

COOPER, S. D., L. BARMUTA, O. SARNELLE, K. KRATZ, AND S. DIEHL. 1997. Quantifying spatial heterogeneity in streams. Journal of the North American Benthological Society 16:174–188.

DAWSON, F. H. 1981. An inexpensive photosynthetic irradiance sensor for ecological field studies. Hydrobiologia 77:71–76.

FEMINELLA, J. W., M. E. POWER, AND V. H. RESH. 1989. Periphyton responses to invertebrate grazing and riparian canopy in three northern California coastal streams. Freshwater Biology 22:445–457.

GUTSCHICK, V. P., M. H. BARRON, D. A. WAECHTER, AND M. A. WOLF. 1985. Portable monitor for solar radiation that accumulates irradiance histograms for 32 leaf-mounted sensors. Agricultural and Forest Meteorology 33:281–290.

HILL, W. 1996. Effects of light. Pages 121–148 *in* R. J. Stevenson, M. L. Bothwell, and R. L. Lowe (editors). Algal ecology: freshwater benthic ecosystems. Academic Press, San Diego.

HILL, W. R., M. G. RYON, AND E. M. SCHILLING. 1995. Light limitation in a stream ecosystem: responses by primary producers and consumers. Ecology 76:1297–1309.

JOHNSON, N. L., S. KOTZ, AND N. BALAKRISHNAN. 1994. Continuous univariate distributions. 2nd edition. John Wiley and Sons, New York.

PAYNE, R. W. (EDITOR). 2000. The guide to Genstat. Part 2: statistics. VSN International Ltd, Oxford, UK.

PEARCY, R. W. 1989. Radiation and light measure-

ments. Pages 97–116 *in* R. W. Pearcy, J. Ehleringer, H. A. Mooney, and P. W. Rundel (editors). Plant physiological ecology: field methods and instrumentation. Chapman and Hall, London, UK.

PONTAILLER, J. Y. 1990. A cheap quantum sensor using a gallium arsenide photodiode. Functional Ecology 4:591–596.

PONTAILLER, J. Y., AND B. GENTY. 1996. A simple red-far-red sensor using gallium arsenide phosphide detectors. Functional Ecology 10:535–540.

UNDERWOOD, A. J., AND M. G. CHAPMAN. 1996. Scales of spatial patterns of distribution of intertidal invertebrates. Oecologia (Berlin) 107:212–224.

VANNOTE, R. L., G. W. MINSHALL, K. W. CUMMINS, J. R. SEDELL, AND C. E. CUSHING. 1980. The river continuum concept. Canadian Journal of Fisheries and Aquatic Sciences 37:130–137.

WOOTTON, J. T., AND M. E. POWER. 1993. Productivity, consumers, and the structure of a river food chain. Proceedings of the National Academy of Sciences of the United States of America 90:1384–1387.

Received: 18 June 2001
Accepted: 14 November 2002